Drug Development and Industrial Pharmacy, 32:185–196, 2006

ISSN: 0363-9045 print / 1520-5762 online
DOI: 10.1080/03639040500466122

Taylor & Francis

Physical Characterization of Anhydrous and Hydrous Forms of the Hydrochloride Salt of BVT.5182 A Novel 5-HT_6 Receptor Antagonist

Andreas Hugerth, Magnus Brisander, Ulla Wrange, Mikael Kritikos, Björn Norrlind, Marianne Svensson, and Mikael Bisrat
Biovitrum AB, Preclinical R&D, Pharmaceutics, SE-112 76 Stockholm, Sweden

Jan Östelius
Biovitrum AB, Preclinical R&D, Analytical Sciences, SE-112 76 Stockholm, Sweden

ABSTRACT The physicochemical properties of 1-benzenesulfonyl-4-(piperazin-1-yl)-indole hydrochloride, a novel 5-HT_6 receptor antagonist for the treatment of obesity were characterized. Two solid state forms were identified at ambient conditions (23°C): an anhydrate form (1) and a hydrate form (2), with 1.5 moles of H_2O. The latter easily dehydrates and rehydrates without affecting the crystal morphology. Investigations of the propensity for interconversion between the two forms reveal that a) conversion of 2→1 takes place above 145°C and that b) conversion of 1→2 only occurs after crystallization from supersaturated aqueous solutions at a water activity ≥0.94 or in the presence of comparable amounts of crystals of 2 in water at ambient conditions. However, in an equimolar suspension of 1 and 2 at 37°C no phase transformation was observed. Thus, the difference in chemical potential between the two forms is small. Form 1 was shown to have overall favorable solid state properties and, hence, considered the preferred form for continued pharmaceutical development. The characterization was performed by means of light microscopy, scanning electron microscopy, powder X-ray diffraction, FTIR/NIR-spectroscopy, differential scanning calorimetry, hot stage microscopy, thermogravimetry, dynamic vapor sorption, Karl Fischer water content determination, phase stability studies of suspensions, solubility, and intrinsic dissolution rate measurements.

KEYWORDS Anhydrate, Hydrate, Solid state characterization, Thermal analysis, 5-HT_6 receptor antagonist

INTRODUCTION

1-Benzenesulfonyl-4-(piperazin-1-yl)-indole (BVT.5182) is a novel potential candidate drug that is a highly potent and selective 5-HT_6 receptor antagonist (Woolley et al., 2004) investigated for the treatment of obesity. The molecular formula of the hydrochloride salt of BVT.5182 is $C_{18}H_{19}N_3O_2S{\cdot}HCl$ and its chemical structure is shown in Fig. 1. The objective of this study was to

Address correspondence to Andreas Hugerth, Pfizer Health AB, Pfizer Consumer Healthcare R&D, Formulation Development, Box 941, SE-251 09 Helsingborg, Sweden; Tel: +46 42 288623; Fax: +46 42 288389; E-mail: andreas.hugerth@pfizer.com

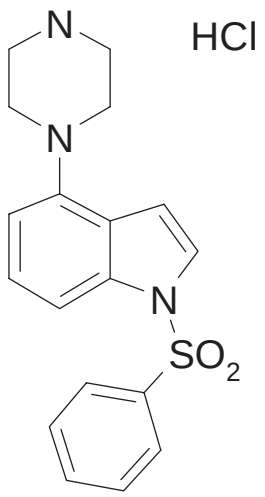

FIGURE 1 **Chemical Structure of BVT.5182 Hydrochloride.**

provide an initial characterization of the physical properties and solid state stability of BVT.5182·HCl. The reason being that it is well known that hydrates/solvates and polymorphs may differ with respect to their physical properties such as solubility, dissolution rate, melting point, hygroscopicity, and stability, thus potentially affecting the bioavailability and the safety of the administered drug (Byrn et al., 1999; Morris & Rodriguez-Hornedo, 1992; Vippagunta et al., 2001). Hence, characterization of solid state and physicochemical properties including possible solvate formation and polymorphism of a novel potential drug candidate is essential for the pharmaceutical development of a new drug substance. The propensity for hydrate formation, the properties of any hydrous forms, and the relationship between the anhydrous and hydrous forms are of special interest since the drug substance often comes in contact with an aqueous environment in pharmaceutical manufacturing processes (e.g., in wet granulation) and during storage.

MATERIALS AND METHODS

Materials

Ethanol was added to the free base followed by heating the solution to 72°C for the preparation of the anhydrous BVT.5182 HCl (1). Subsequent addition of concentrated hydrochloric acid followed by seeding with 1 initiated the crystallization of 1. After cooling to 3°C, the product was isolated on a Nutsche filter. The product cake was washed with ethanol and dried at 80°C and under vacuum. The material was produced by the Chemical Process Development Department at Biovitrum.

The hydrate form of BVT.5182·HCl (2) was prepared by dissolving 200 mg of 1 in 7.0 mL purified water at 70°C. The solution was filtered through a solvent resistant filter (pore size 0.45 μm, Sartorius, minisart srp 15) and then cooled to room temperature. No crystals were formed during the cooling process, but were formed after being kept at room temperature for 3 h followed by cooling to 4°C for 1 h. Excess water was removed overnight by vacuum drying.

Recrystallizations of 1 from methanol–water mixtures (in the interval 5–95% w/w) were performed by dissolving ca 40 mg of 1 in a minimal volume of solvent at 55°C. The solutions were placed at ambient temperature (23 ± 1°C) overnight, and the formed crystals were collected and dried at ambient conditions. All chemicals used were of analytical grade.

Methods

Microscopy

Transmission light microscopy (LM) and hot stage microscopy (HSM) studies were performed on a Zeiss Axioplan microscope equipped with polarizing filters and a Linkam THMS600/TMS 92 Hot Stage (×10 objective). The heating rate for the HSM was 3K/min in air and $N_{2(g)}$, respectively.

Scanning electron microscopy (SEM) was performed with a digitized SEM (JEOL T-200, Tokyo, Japan) operated at a 5–15 kV accelerating voltage. The samples were placed on a metal stub with double-sided adhesive tape, and coated with gold under reduced pressure.

Differential Scanning Calorimetry (DSC) and Thermogravimetry (TG)

Differential Scanning Calorimetry (DSC) and TG were run on a Mettler DSC30 and a Mettler TG50 with a Mettler M15 microbalance, respectively, connected to a TA controller unit, TC10A/TC15, (Mettler Toledo, Grefensee, Switzerland). Analysis was performed using STAR^e 5.0 software. For the DSC, samples of 2–4 mg were weighed into 40 μl Al pans, which were generally punctured (unless otherwise noted). Samples for TG (approximately 10 mg) were weighed into open 70 μl Pt-pans. The standard heating

rate was 10 K/min with a nitrogen flow of 50 mL/min and 200 mL/min for the DSC and TG, respectively. Synthetic air of scientific quality was used in some experiments. This gas mixture was provided by Linde Gas (AGA). It is produced by mixing pure oxygen (20%) and pure nitrogen (80%), quality code 5.5 (water content ≤2 ppm).

Powder X-ray Diffraction (PXRD)

Powder X-ray diffraction (PXRD) was performed at ambient conditions on a SCINTAG X'TRA (Thermo ARL, Ecublens, Switzerland), using Cu K_α radiation (45 kV and 40 mA) and a Peltier-cooled silicon detector.

Data were collected in step scan mode in the range 2–60° 2θ with a step size of 0.01° 2θ, preset time 2.0 seconds. The slit of the tube divergent, tube scatter, detector scatter, and detector reference was 2.0, 4.0, 0.5, and 0.2 mm, respectively.

Standard reference material 675 (Mica, fluorophlogopite) from the National Bureau of Standards was added as an internal standard to correct for systematic errors in the low 2θ region. Data collections were preformed with DMSNT Version 1.50-Beta software (Thermo ARL, Switzerland) and the pattern analysis, including indexation, was made with JADE 6+ (Materials Data, Inc., Livermore, CA, USA) and the KOHL (Kohlbeck & Hörl, 1976, 1978) and TREOR90 (Werner et al., 1985) programs in the CRYSFIRE System for Automatic Powder Indexing (Shirley, 2004). The unit cell parameters were refined with the program PIRUM (Version 930101) (Werner, 1969).

Fourier Transform Infrared Spectroscopy (FTIR)

Mid-FTIR (4000–400 cm^{-1}) spectra were obtained in the transmission mode with KBr disk (0.3% w/w sample) on a Perkin-Elmer 2000. FTIR-microscopy (4000–400 cm^{-1}) and NIR-spectra (8000–4000 cm^{-1}) were obtained in the diffuse reflectance mode.

Dynamic Vapor Sorption Gravimetry (DVS)

The hygroscopicity of the samples was studied by a Dynamic Vapor Sorption gravimetry (DVS) instrument, (DVS-1, Surface Measurement Ltd., London, UK). The samples were placed in the chamber at an initial relative humidity (RH) of 30%. The relative weight change of samples (~10 mg) was continuously recorded at 25.0 ± 0.1°C as the target RH was cycled stepwise from 0–98% or 0–90% and then back. Each experiment was run in three consecutive full cycles. The limiting condition for proceeding to the next level of RH was a weight increase below 0.001% per 20 seconds, within 15 min to 24 h.

Karl Fischer Water Content Determination (KFT)

The water content of samples of 1 and 2 (10–20 mg) in anhydrous methanol was determined using a Mettler DL18 (Mettler Toledo, Grefensee, Switzerland). Samples were analyzed in duplicate (Mikro Kemi AB, Uppsala, Sweden).

Solubility

The solubility was determined by use of a HPLC-system, with two Shimadzu LC-10ADvp HPLC-pumps, a SPD-10Avp Shimadzu UV-(VIS) detector, a SIL-10ADvp Shimadzu autoinjector, a CTO-10ASvp Shimadzu column oven, and a SCL-10Avp Shimadzu system controller. The data were evaluated with Millennium 32 ™Waters Chromatography Data System. An Xterra™ MS C18, 50 × 2.1 mm column with a mean particle size of 3.5 µm was used for all measurements. The mobile phase consisted of acetonitrile, water, and trifluoroacetic acid, 5:95:0.1(A) and 99:1:0.1(B). A gradient profile where the mobile phase B content was increased from 20% to 100% during 3 min was followed by 100% B for 2 min and finally 20% B for 2 min. A flow rate of 0.4 mL/min, UV-detection at 266 nm, column temperature at 30°C, and injection volume of 5 µl were used.

An excess amount of substance was weighed in vials and 0.5 mL or 2.0 mL of the media; simulated gastric fluid without enzymes, SGF (pH 1.3), and intestinal gastric fluid without enzymes, SIF (pH 6.7), prepared according to USP 24. 0.15 M phosphate buffer (pH 6.9), 0.15 M phosphate buffer (pH 10.7), 0.05 M, 0.10 M, 0.15 M, 0.5 M of $NaNO_3$ and 0.05 M, 0.10 M, 0.15 M, 0.5 M of NaCl was added. The substance and the specific media were rotated in vials using a rotation board or stirred with a magnetic bar at ambient conditions for 24 h. Rotation of the samples for an additional 3 days did not produce any changes in the solubility. Excess substance was filtered using a

hydrophilic PVDF 0.22 μm filter and the pH of the collected filtrate was measured. The samples were then diluted in a range of 1:2 to 1:200 with a 1:1 mixture of mobile phase A and B. The solubility was calculated from a calibration curve obtained by analyzing samples with known concentrations.

Intrinsic Dissolution Rate (IDR)

The intrinsic dissolution rate (IDR) studies were carried out by means of a rotating disc method (Wood Intrinsic Apparatus, VanKel, NC, USA) according to USP XXV (U.S. Pharmacopoeia, 2002). A powder sample, approximately 30–50 mg, was compacted into a tablet with an area 0.5 cm^2 in a stainless steel holder. The holder shaft was mounted into a dissolution tester and immersed in 500 mL simulated gastric fluid, without enzyme (SGF, pH 1.2), or simulated intestinal fluid, without enzyme (SIF, pH 6.7), at 37°C and the rotation speed was set to 100 rpm. Samples (1.0 mL) for concentration determination of the dissolved compound were taken at regular intervals during a period of approximately 8 h. The cumulative amount dissolved per unit area is given by the cumulative amount dissolved at each time point, corrected for sampling losses, and divided by the surface area exposed (0.5 cm^2). The intrinsic dissolution rate of the sample, (in mg/min/cm^2), was given by the slope of the linear least-squares regression line which was fitted to the data points.

Analysis of Degraded Samples

Samples to be analyzed for possible degradation were extracted from DSC pans in a H_2O:ethanol (50:50) mixture, which was subjected to sonication (2 h) and magnetic stirring overnight. The samples were analyzed by means of HPLC (vide supra) on an Xterra™ MS C18, 50 × 2.1 mm column at 220 nm using a gradient profile with a linear increase during 25 min of mobile phase B (see Solubility previously mentioned) from 5 % to 100%.

RESULTS AND DISCUSSION

Microscopic and Visual Observations

Form 1 appeared as a slightly yellow-brownish powder with plate/columnar shaped crystals with varying degrees of agglomeration while the crystals of 2 were mainly acicular (Fig. 2). Both forms displayed birefringence in the polarized light microscope, indicating the samples to be crystalline (Fig. 2b and 2d).

Water Content and Hygroscopicity

The water content of 2 was 6.5% w/w as given by KFT. This result indicates it to have a molar stoichiometric ratio of approximately 1.5 mol H_2O per mol BVT.5182 HCl, hence it will tentatively be referred to as a sesquihydrate. Dynamic vapor sorption (DVS) results showed 2 to have a relative weight loss of approximately 6% w/w as it was dried at 0% RH prior to the start of the DVS run, which most probably was associated with loss of water, thereby supporting the KFT finding. Further information on the water content and the hygroscopicity of 2 is given by the moisture sorption/desorption profiles shown in Fig. 3. The sorption profile of 2 shows a major one step weight increase in the interval 5–10% RH which levels out at 10–20% RH. Thus, the dehydrated 2 sample readily reabsorbs moisture already at low relative humidity. In the interval 20–90% RH, the weight increased from 5.9% to 6.6%. Thus, in the given RH range DVS indicates the molar ratio to vary between 1.3–1.5 mol H_2O per mol BVT.5182. The desorption curve shows a minute hysteresis above approximately 10% RH but below this value the hysteresis is pronounced. At the end of the cycle, the desorption curve returns to a value practically coinciding with the initial weight of the sample at 0% RH. After the initial RH cycle, the sample was subjected to two subsequent cycles resulting in practically identical sorption–desorption isotherms. Powder x-ray diffraction (PXRD) did not indicate any phase change of the sample after the DVS run relative to the starting material and, hence, a crystal structure of 2 that is unchanged after rehydration. Thus, the shapes of the DVS isotherms are suggestive of a stoichiometric hydrate with channel-type water of hydration.

Karl Fischer water content determination (KFT) indicated the water content of 1 to be 0.5% w/w. For the anhydrate form, the sorption curve in the DVS showed a steady but small increase in weight as the sample was exposed to progressively higher relative humidity in the range 0–98% RH (Fig. 3). The relative weight gain of approximately 0.25% at 98% RH can be attributed to surface adsorbed water and possibly also moisture adsorbed to a minor amorphous or disordered component. The desorption curve shows a minor hysteresis but returns at the end of the cycle to

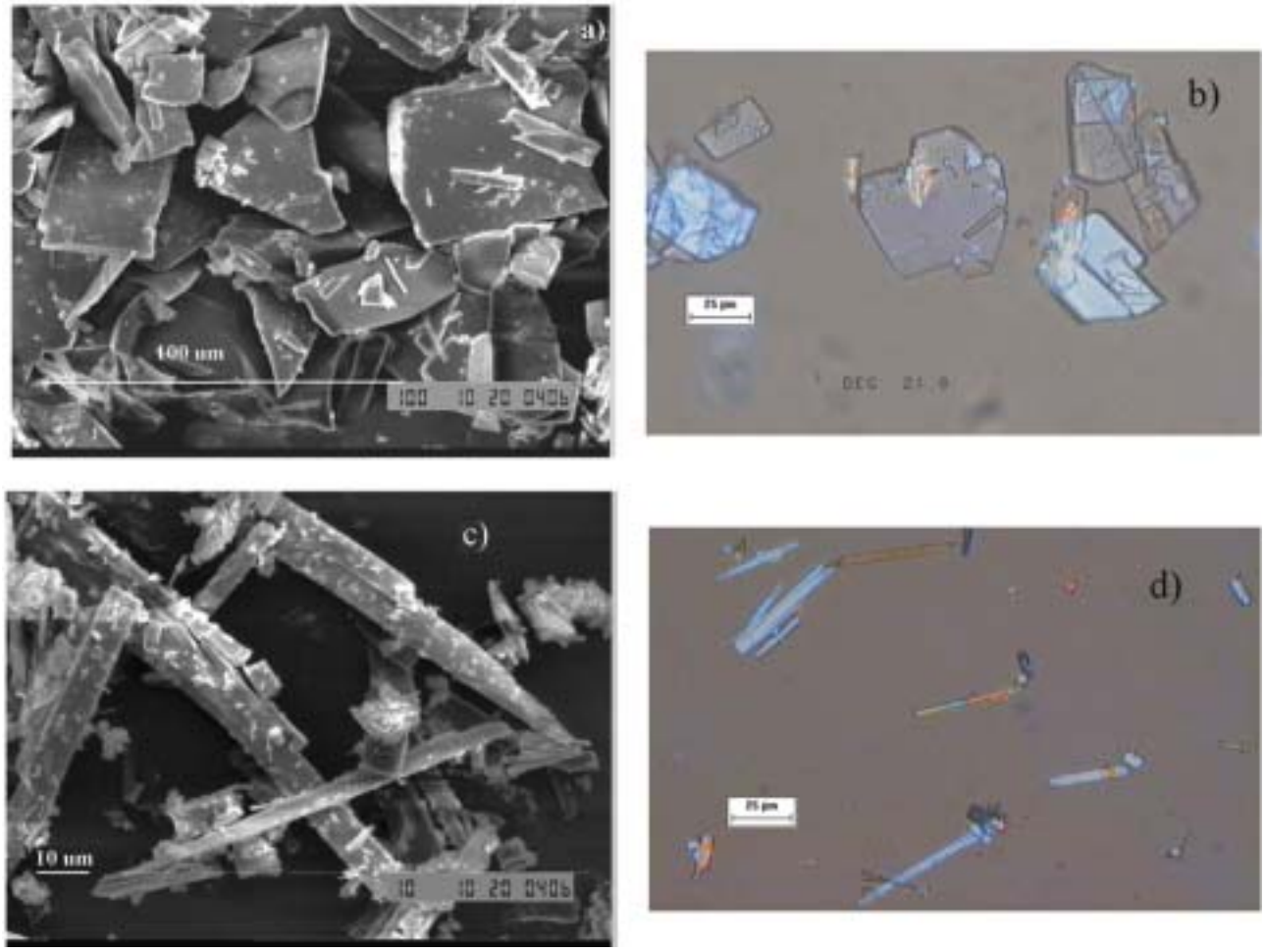

FIGURE 2 **SEM and Transmission Light Micrographs of Form (a, b) and Form (c, d).**

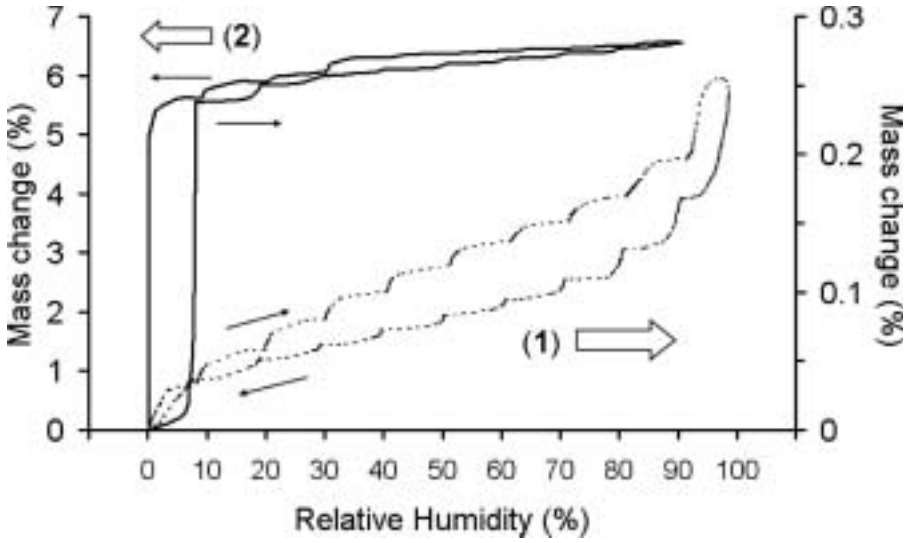

FIGURE 3 **The Relative Change in Mass as Function of Relative Humidity at 25°C by Means of DVS of 1 (Dotted Line and Right Axis) and 2 (Solid Line and Left Axis).**

a value practically coinciding with the initial weight at 0% RH. Hence, there was no indication of any conversion of the anhydrate to a hydrate form during the DVS experiment.

Powder X-ray Diffraction and Infrared Spectroscopy

The powder x-ray diffraction (PXRD) patterns of 1 and 2 are shown in Fig. 4. The rather narrow diffraction peaks and low background of the diffraction profiles indicated the samples to be predominately crystalline, hence substantiating the microscopy findings. The distinctly different PXRD pattern of 1 compared to that of 2 shows the anhydrate and hydrate forms to be two separate phases. Arrows in Fig. 4 denote some of the major differences. Indexation of the PXRD pattern of 1 indicated it to be primitive monoclinic with the cell dimensions a = 18.652(5) Å, b = 6.068(2) Å, and c = 16.023(4) Å, β = 94.75(3)° with a unit cell volume of 1807(1) Å^3, and a calculated density of 1.267(2) g/cm^3 (Z = 4). Form 2, was also indexed as primitive monoclinic with the cell dimensions a = 38.486(16) Å, b = 12.031(3) Å, and c = 8.562(3) Å, β = 92.83(4)° with a unit cell volume of 3960(4) Å^3.

There were some distinct differences between the FTIR spectra of the hydrate compared to the anhydrate (Fig. 5). The most significant difference is the broad and shouldered absorption band of 2 at 3600–3200 cm^{-1} corresponding to the O–H stretching region, which is practically absent in the spectrum of 1. This is indicative of a hydrate since hydrates usually have an absorption band at 3600–3100 cm^{-1} (ν_{OH}) (Nakanishi, 1962; Socrates, 1994). The broadness of the peak and its shouldered shape may indicate the water molecules may have different types of binding and, hence, occupy a number of different positions in the crystal structure of 2 rather than to occupy one discrete part of the crystal lattice (Zhu et al., 1997a). The shape of the spectra of individual crystals of the anhydrate and hydrate form obtained by FTIR microscopy agreed with the spectra obtained by the KBr disk method, albeit with a lower signal-to-noise ratio. It could thus be shown that the pressure applied during the preparation of the KBr disks did not produce any structural change observable by FTIR. NIR spectra of untreated 2 showed a large broad absorption band at 4900–5300 cm^{-1} with a peak at 5046 cm^{-1}, which was essentially absent in the spectra of 1 and is indicative of a hydrate (-OH vibration 5130 cm^{-1}), thereby substantiating the FTIR findings.

Thermal Analytical Studies

Thermal Properties of the Anhydrate (1)

The thermal properties of 1 are shown in Figs. 6, 7, and 8. The DSC curve of the anhydrous form shows a single melting endotherm in the temperature range

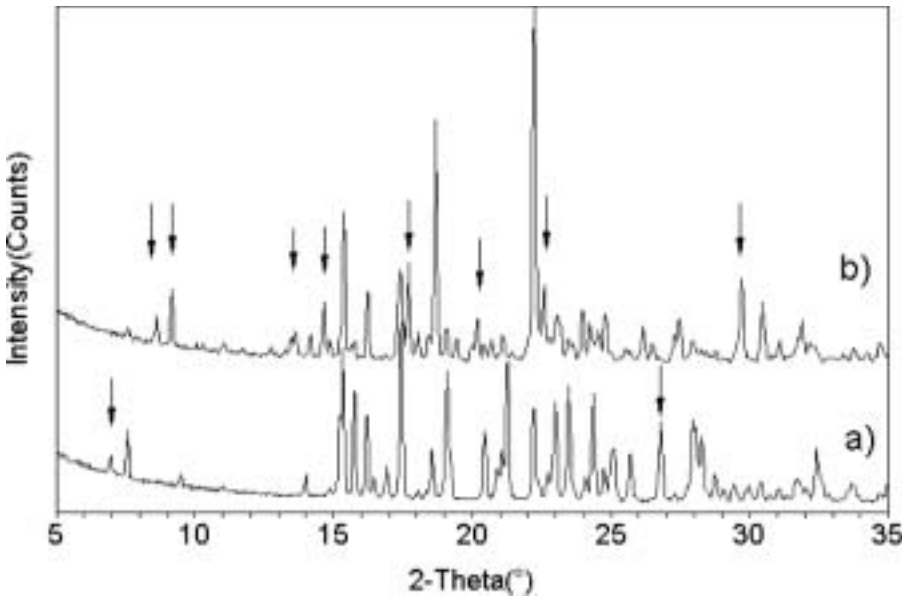

FIGURE 4 **Powder X-ray Diffractograms of a) 1 and b) 2.**

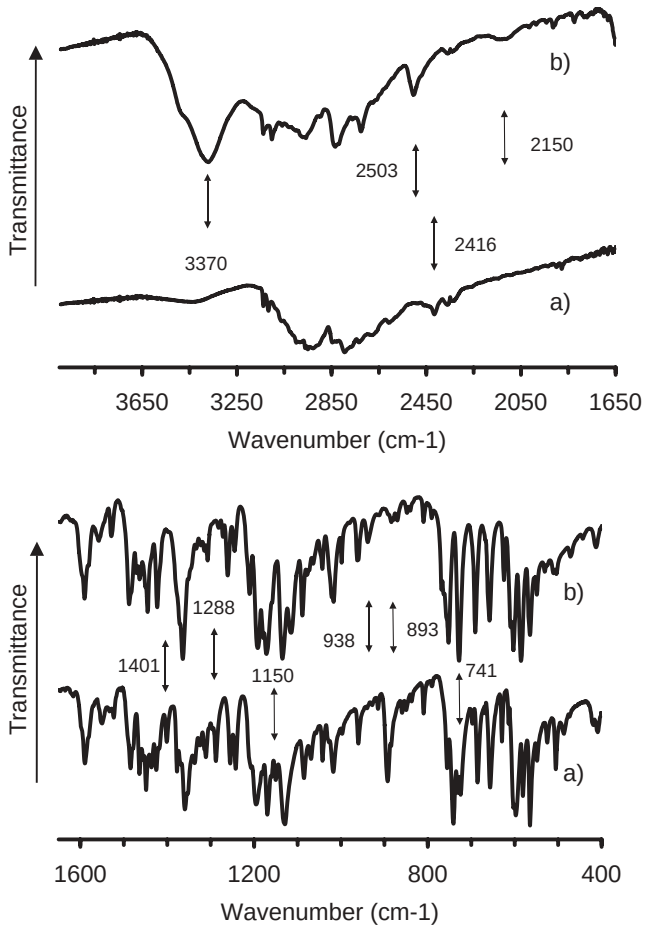

FIGURE 5 **FTIR Spectra of a) Form 1 and b) Form 2.**

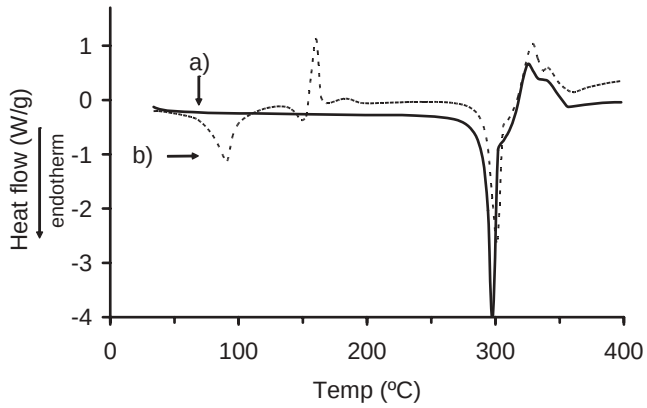

FIGURE 6 **DSC Curves of a) Form 1 and b) Form 2.**

250–315°C, with an extrapolated melting temperature onset of 293.6 ± 0.9°C (n = 5), a peak temperature of 298.8 ± 0.6°C (n = 5), and an enthalpy of fusion of 153 ± 10 kJmol^{-1} (n = 5). The melting endotherm was followed by an exotherm suggestive of decomposition.

Prior to the melting/decomposition event, the TG showed a weight loss of <0.6% from 30 to 230°C. HPLC analysis of a sample 1 heated to 230°C in the DSC and subsequently allowed to cool to ambient temperature did not indicate any decomposition. The observed weight loss is therefore probably due to loss of surface adsorbed moisture and residual organic solvents. The TG also showed a further weight loss of 0.9% in the temperature range 230 to 260°C, which may be related to decomposition. Concomitant with the melting process, the TG signal indicated a major weight loss. This, together with the HSM findings, indicate 1 to be unstable during melting. HPLC analysis of a sample of 1 heated to 300°C in the DSC confirmed the suspected decomposition (approximately 10%). These findings show that the value given above for the enthalpy of fusion for the anhydrate is flawed and should be regarded as indicative only of its order of magnitude. Furthermore, a sample heated to 330°C in the DSC was shown by HPLC analysis to contain only approximately 20% of form 1. Hence, the exothermic event following the melting endotherm can unequivocally be ascribed to sample decomposition.

Further DSC studies of 1 supported the HSM finding of differences in the thermal behavior of 1 in the presence of air compared to nitrogen. Differential scanning microscopy (DSC) runs in air were preformed in punctured Al pans at various heating rates in the range 1–30 K/min (Fig. 7). At the lower heating rates (1 K/min and 3 K/min), the melting endotherm is virtually obscured by the exothermic events indicated in the DSC curve. At the higher heating rates (10 K/min and 30 K/min), exothermic events are observed both before and after the melting endotherm. In comparison, exothermic events are evident mainly after the melting endotherm when a nitrogen atmosphere is used. A similar thermal behavior has previously been observed for retinoic acid (Berbenni et al., 2001) and ranitidine hydrochloride (Marti et al., 2000).

Thermal Properties of the Hydrate (2)

With respect to 2, the DSC curve is more complex (Fig. 6). The endothermic event in the temperature range 40–120°C was accompanied by a one-step-weight loss (3.3%) in the TG (Fig. 8), indicative of solvent evaporation. However, the initial water content was in excess of 3.3%, as given by KFT results, DVS data, and by a subsequent TG experiment where 2 lost 5.3% after 10 min at 40°C. The variation in weight loss observed for 2 in the TG experiments was related

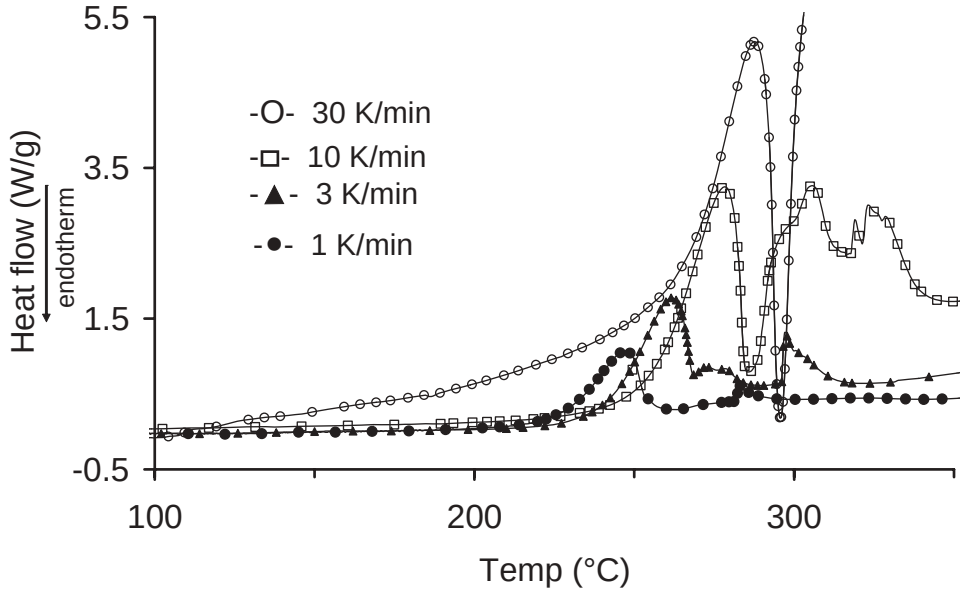

FIGURE 7 **DSC Curves of 1 in Synthetic Air at Different Heating Rates. (Some of the Measuring Points Are Shown as Markers as a Guide to the Eye).**

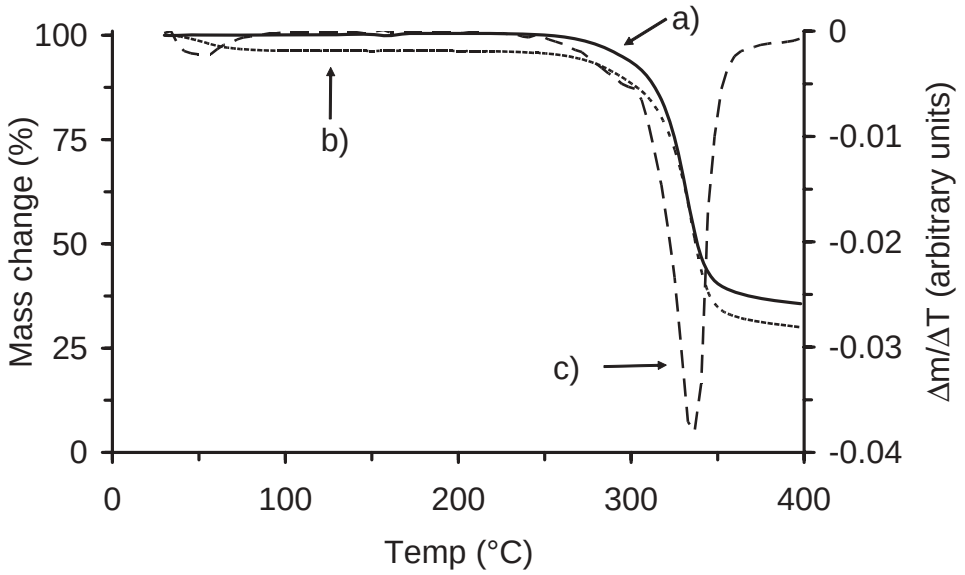

FIGURE 8 **TG Curves of a) 1, b) 2, and c) the First Derivative of the TG Curve of 1.**

to the dry nitrogen purge. The heat of vaporization of water and the heat associated with the release of water from the crystal lattice (ΔH_{WCL}) of 2 was 45 ± 10 kJ·mol^{-1} (n = 3), which is of the same order as the heat of vaporization of pure water (ΔH_{PW} = 40.7 kJ·mol^{-1}), and corresponds to approximately two hydrogen bonds per water molecule (Zografi, 1988). The given ΔH_W value is ~20 % less than that reported for the H_2O–Tetroxoprim system, which was found to have a sharp desolvation endotherm in the DSC curve and it was concluded that the water is located in isolated sites in the crystal (Caira et al., 2002). Thus, the interaction between H_2O and the BVT.5182 molecules seems to be relatively weak as indicated by the low temperature onset of the dehydration event, the broad dehydration endotherm, the given ΔH_{WCL} value, and the ease of evaporation in the TG experiment (Perrier & Bryn, 1982). In addition, the broad dehydration endotherm, together with the FTIR results, indicates the energies of association of the water bonds in 2 to

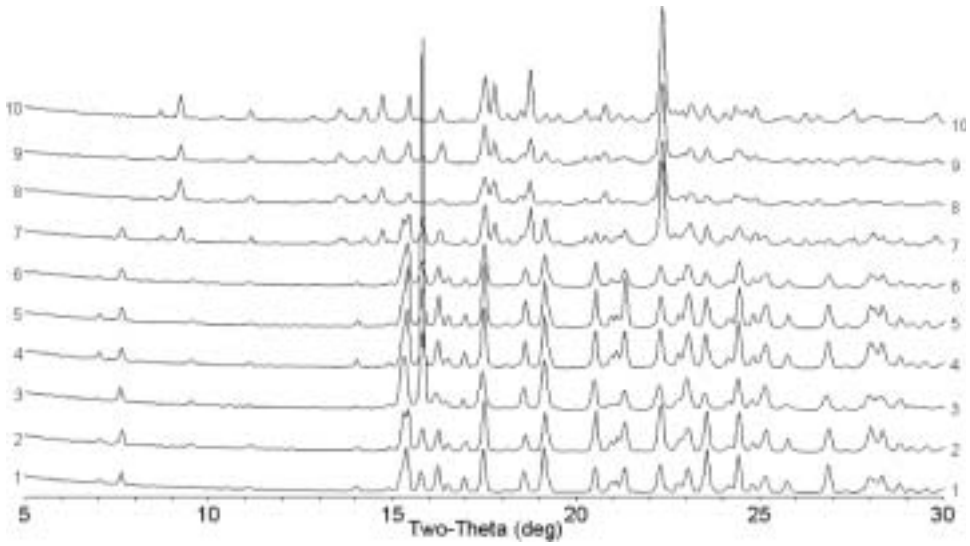

FIGURE 9 **Powder X-ray Diffractograms of 1 Stored at 40°C/75% RH for 3 Months (1), 40°C/90% RH for 1 Month (2), form 2 After Heating to 225°C (3), Simulated Granulation in H_2O 10% w/w (4), Suspension of Anhydrate After Solubility Studies Stored $3^1/_2$ Months at 23°C (5), Anhydrate Suspension Seeded with Form 2 Stirred 24 hr at 23°C (6), Equimolar Suspension of 1 and 2 Stored 1 Month at 37°C (7), Equimolar Suspension of 1 and 2 Stored 1 month at 23°C (8), Equimolar Suspension of 1 and 2 Stirred 24 Month at 23°C (9), Suspension of Hydrate After Solubility Studies Stored $3^1/_2$Months (10), Respectively.**

encompass a wide distribution. Moreover, HSM did not indicate any change in the habit of 2 in the temperature range corresponding to the evaporation of water as given by TG and DSC. In fact, no change in the morphology could even be observed when 2 was heated to 60, 85, 100, and 115°C, and the temperature maintained for 120 min. Taken together, these results are, as the DVS data, suggestive of a structure where (some of) the water molecules are located in a channel/tubular structure.

After the initial solvent evaporation there were no observable thermal events as indicated by DSC and TG in the temperature range 115–145°C. Thus, in this temperature interval, an anhydrous form of 2 seems to be present. This possible polymorph of 1 was tentatively designated as 1:II; a finding that should ideally be confirmed by an experiment such as variable temperature PXRD with 2. Following the previously given temperature interval, there is a complex series of thermal events in the temperature range 145–200°C, which includes an endotherm with peak temperature at 149.1 ± 1.3°C (n = 3), an exotherm with peak temperature at 158.0 ± 1.7°C (n = 3) and a rather broad but small exothermic event with a peak temperature of ~185°C. Hot stage microscopy (HSM) experiments supported the DSC findings. The endothermic process is possibly due to a collapse/melting of the structure and the following exothermic processes can be ascribed to recrystallization/rearrangement resulting in the formation of a more stable anhydrous crystal form of 2. The melting with decomposition of the more stable form with an extrapolated melting temperature onset of 294.6 ± 1.6°C (n = 3) and a peak temperature of 299.8 ± 0.9°C (n = 3) practically coincides with that of the anhydrate (1). An experiment where 2 was heated in a pierced Al pan in the DSC from 30°C to 225°C at 10 K/min and then cooled to 30°C at 50 K/min, showed that the derived sample had the same PXRD diffractogram (Fig. 9) as the anhydrate 1. Hence, the series of thermal events evident in the temperature range 115–200°C represents an irreversible phase transition from a metastable anhydrous form of 2 (1:II) to the anhydrous phase that constitutes 1.

Solubility and Intrinsic Dissolution Rate

The pKa value of BVT.5182 is 8.9 (Gäfvert, 2003). Thus, in all solubility measurements performed at a pH close to or below 7, the salt BVT.5182. HCl is predominantly present in a dissociated ionic state. The solubility of 1 and 2 in water at ambient conditions was 3.71 ± 0.06 (n = 3, pH 6.5) and 4.00 ± 0.02 mg/mL (n = 3, pH 6.5), respectively. Both forms can thus be classified as slightly soluble. However, the use of magnetic stirring instead of rotation resulted in a

solubility of 5.33 ± 0.06 mg/mL (n = 3, pH 6.2) for 1 and 4.88 ± 0.06 mg/mL (n = 3, pH 6.4) for 2 (at 23 ± 1°C). The results from both methods were reproducible and the solubility values did not change with time (3 days). The small difference in solubility between the anhydrate and hydrate form and the reversal of order suggests the difference in chemical potential between them to be rather small. The solubility of 1 was also studied (in duplicate) in simulated gastric fluid (SGF, pH 1.3), simulated intestinal fluid (SIF, pH 6.7), and 0.15 M phosphate buffer (pH 6.9) and was found to be 0.53, 0.37, and 0.31 mg/mL, respectively. The solubility in 0.15 M phosphate buffer at pH 10.7, where BVT.5182 is present predominately as free base, was 0.08 mg/ml. The given solubility results, combined with additional solubility studies of 1 in $NaCl_{(aq)}$, and $NaNO_{3(aq)}$ (Table 1.), indicate the solubility to be dependent not only on pH but also on ionic strength. However, there was no indication of a common ion effect with respect to chloride.

The intrinsic dissolution rate of 2 at 37°C in SIF (pH 6.8) was 0.02 mg/cm^2/min and 0.003 mg/cm^2/min for form 1, and hence both forms dissolve slowly. For 1 the IDR in SGF (pH 1.2) was 0.04 mg/cm^2/min (single measurement). The phase of the remaining anhydrate compact was shown by PXRD not to have changed during the IDR experiment. The free energy of hydration (ΔG_h = 4.89 kJ/mol) at constant temperature and pressure was obtained from the intrinsic dissolution rates of the anhydrous and hydrous forms according to:

$$\Delta G_h = RT \ln(IDR_{hydrate}/IDR_{anhydrate}) \qquad (1)$$

TABLE 1 Solubility of BVT.5182 HCl in the Presence of $NaNO_3$ and NaCl, Respectively

Solvent*	Solubility mg/ml**
$NaNO_3$ (0.05 M)	0.42 (6.5)
$NaNO_3$ (0.10 M)	0.23 (7.1)
$NaNO_3$ (0.15 M)	0.16 (6.9)
$NaNO_3$ (0.50 M)	0.07 (7.1)
NaCl (0.05 M)	0.73 (5.3)
NaCl (0.10 M)	0.44 (6.0)
NaCl (0.15 M)	0.34 (6.4)
NaCl (0.50 M)	0.14 (6.4)

*Ionic strength due to NaCl or $NaNO_3$ given in parenthesis. Contribution of **1** or **2** to the ionic strength is not included.

**pH of solution after equilibration given in parenthesis.

This equation is valid under certain conditions (that are valid in our system). The dissolution process of hydrate and anhydrate solid, respectively, give the same molecular species in the solution. To a good approximation, this gives the same diffusivity, D, of the dissolved species. In addition, since no reaction takes place the dissolution step is transport controlled. We can then assume that the thickness of the diffusion layer, h, is of equal magnitude in the two cases. If both D and h are constants, we have constant hydrodynamic conditions. Finally, this means that the dissolution rate constant, k, which depends on the factor D/h, adopts the same value for the hydrate and the anhydrate. The remaining variable affecting the dissolution rate is then the intrinsic solubility of the material.

The obtained rank order in SIF at 37°C, $IDR_2 > IDR_1$, results in a positive free energy of hydration in this case, indicating the anhydrate to be more stable in water than the hydrate at 37°C. This is the opposite of what is normally found since hydration processes are usually accompanied by a free energy decrease (Vippagunta, 2001). However, a similar finding has been reported by Reutzel-Edens (Reutzel-Edens et al., 2003).

Stability in Solid State and in Solution

Simple simulated granulation experiments with form 1 in 10–50 % w/w H_2O was shown by PXRD diffractograms to have no effect on the phase of 1 (Fig. 9). Furthermore, PXRD analysis of the remaining solid material of 1 and 2 obtained from the saturated aqueous solutions in the solubility experiment, and hence with a water activity close to unity which had been stored as suspensions at ambient temperature for 3½ months, did not indicate any phase changes to have occurred (Fig. 9). Hence, any conversion from 1 to 2 or another hydrate form was not sufficiently thermodynamically or kinetically favorable for conversion to occur within the given time period. This result obtained in solution corresponds to that indicated by the DVS experiment which is a semi-equilibrium method where phase transformation mainly is mediated in the vapor phase.

In an attempt to further investigate which form is the most stable at ambient conditions and at 37°C, equimolar suspensions of 1 and 2 were prepared and

magnetically stirred for one month and subsequently vacuum dried. A justification of this method for determining the relative stability of an anhydrate and a hydrate was recently described by Sacchetti (Sacchetti, 2004). Powder x-ray diffraction (PXRD) diffractograms showed that the collected solid material, which had been stored at ambient conditions (Fig. 9), was identical to 2 whereas both forms were present in the suspension that had been stored at 37°C (Fig. 9). Furthermore, PXRD of an equimolar suspension of 1 and 2 stirred only 24 h at ambient conditions (Fig. 9) also had the same phase as 2 while there was no indication of any transformation to have occurred in a suspension of 1 that only had been seeded with 2 and stirred 24 h (Fig. 9). Thus, that the conversion from 1→2 at ambient conditions seems to be dependent on the amount of crystals present of 2 for a non-supersaturated solution, indicates the kinetics of the phase transition to be very slow. The result of the suspension experiments suggest that 2 is slightly more stable than 1 at ambient conditions and that they are energetically approximately equally favored at 37°C. This latter result is interesting since both types of crystals were present at water activity close to unity. Moreover, this result can be viewed almost as a limiting case in comparison with studies performed by Zhu et al. (1996) where an equilibrium water activity was found between anhydrous and hydrous forms in the theophylline and the ampicillin systems (Zhu & Grant, 1996).

To further elucidate the relationship between 1 and 2 as well as the propensity of BVT.5182 to form other hydrate/solvate forms or polymorphs, recrystallization in some water-organic solvent mixtures and organic solvents were performed. Recrystallization of 1 from methanol-water mixtures in the interval 5–95% w/w showed that 2 was formed from solutions with ≥90% w/w water ($a_w \geq 0.94$), whereas 1 was obtained from solutions with ≤80% w/w water ($a_w \leq 0.89$), as given by PXRD and DSC. The water activities were calculated according to the formula given by Zhu et al. (1996). These results also indicate the thermodynamically favored form in water at ambient conditions to be 2. Preliminary PXRD and DSC results from recrystallization from ethanol–water mixtures, *n*-propane, and isopropanol did not indicate any solvate formation or polymorphism. In addition, the produced crystals had a different morphology (columnar) when compared to the starting material. These results are of general interest since they show that the kinetics of hydrate–anhydrate phase transformation can be exceedingly slow, and that just seeding may not be sufficient for phase transformation to occur in a system where the difference in the chemical potential between the various crystal forms is very small if not sufficient time is allowed for the transformation. In addition, the results emphasize the importance of not relying on solely solubility or IDR measurements when assessing the stability, for example an anhydrate form versus a hydrate form.

Form 1 was subjected to a solid state stability study since it has more favorable solid state properties. Samples of 1 were exposed to 40°C/90% RH or 40°C/75% RH in open containers for 1 month and 3 months, respectively. Analysis by PXRD (Fig. 9), TG, and DSC of 1 did not, as expected from the results presented (*vide supra*), indicate any phase transitions or degradation under these storage conditions. In addition, tablets of form 1 prepared for IDR and FTIR studies were shown by PXRD to have the same phase both pre- and post-compaction.

CONCLUSIONS

BVT.5182 HCl was found to exist as an anhydrate and as a hydrate with a 1:1.5 molar ratio, which do not readily interconvert at ambient conditions. Form 1 was found to be crystalline, single-phased, and showed good thermal properties, although it was sensitive to degradation in the presence of air at elevated temperatures, and to have low hygroscopicity. Interestingly, 1 was observed to convert to 2 only after crystallization from supersaturated aqueous solutions, $a_w \geq 0.94$, or in the presence of comparable amounts of crystals of 2 in water at ambient conditions. However, in an equimolar suspension of 1 and 2 at 37°C, no phase transformation was observed. The results show that for phase transformation to the most stable form to occur within a reasonable time frame (from a practical point of view) in a system where the difference in chemical potential between the phases is small, large amounts of the thermodynamically most stable form must be present even in a solution-mediated phase transformation. Although 2 was relatively stable in the range 10–90% RH, it easily isomorphically dehydrated/rehydrated at relatively low temperatures and also converted into 1 if heated above 145°C. Interestingly, the overall characteristics of 2 were found to be intermediate between those of a "typical" stoichiometric hydrate and a non-stoichiometric channel structured hydrate.

However, to prevent conversion of 1→2 care should be taken not to expose 1 to 2 during processing in an aqueous environment or long-term storage.

ACKNOWLEDGMENTS

The authors thank Dr. Andrew Browning for his valuable comments on the manuscript. We also thank Dr. Elisabeth Gäfvert for performing the pKa measurement.

REFERENCES

Berbenni, V., Marini, A., Bruni, G., & Cardini, A. (2001). Thermo-analytical and spectroscopic characterization of solid-state retinoic acid. *Int. J. Pharm.*, *221*, 123–141.

Byrn, S. R., Pfeiffer, R. R., & Stowell, J. G. (1999). *Solid-state Chemistry of Drugs* , (2nd Ed.). West Lafayette: SSCI, Inc., 574.

Caira, M. R., Bettinetti, G., & Sorrenti, M. (2002). Structural relationships, thermal properties, and physicochemical characterization of anhydrous and solvated crystalline forms of textroprim. *J. Pharm. Sci.*, *91*, 467–481.

Gäfvert, E. (2003). Internal communication (Measurements performed with Sirius Analytical Instruments Ltd., East Sussex, UK).

Kohlbeck, F., & Hörl, E. M. (1976). Indexing program for powder patterns especially suitable for triclinic, monoclinic, and orthorhombic lattices. *J. Appl. Cryst.*, *9*, 28–33.

Kohlbeck, F., & Hörl, E. M. (1978). Trial and error indexing program for powder patterns of monoclinic substances. *J. Appl. Cryst.*, *11*, 60–61.

Marti, E. E., Kaisersberger, E. W., Kaiser, G. H., & Ma, W.-Y. (2000). *Netzsch annual 2000. Thermoanalytical characterization of pharmaceuticals*, Netzsch-Gerätebau GmbH, Selb, 94–99.

Morris, K. R., & Rodriguez-Hornedo, N. (1992). Hydrates. In *Encyclopedia of Pharmaceutical Technology*, Swarbrick, J., & Boylan, J. C., Eds.; New York: Marcel Dekker Inc., vol. 7, 393–440.

Nakanishi, K. (1962). *Infrared absorption spectroscopy*: Practical, Nankodo Co Ltd, Tokyo, 30 and 210.

Perrier, P. R., & Byrn, S. R. (1982). Influence of crystal packing on the solid-state desolvation of purine and pyrimidine hydrates: Loss of water of crystallization from thymine monohydrate, cystine monohydrate, 5-nitrouracil monohydrate and 2′-deoxyadenosine monohydrate. *J. Org. Chem.*, *47*, 4671–4676.

Reutzel-Edens, S. M., Kleeman, R. L., Lewellen, P. L., Borghese, A. L., & Antoine, L. J. (2003). Crystal form of LY334370 HCl: Isolation, solid-state characterization and physicochemical properties. *J. Pharm. Sci.*, *92*, 1196–1205.

Sacchetti, M. (2004). Determining the relative physical stability of anhydrous and hydrous crystal forms of GW2016. *Int. J. Pharm.*, *273*, 195–202.

Shirley, R. (2004). *The CRYSFIRE System for Automatic Powder Indexing: User's Manual.* 41 Guildford Park Avenue. Surrey, GU2/NL, England: The Lattice Press.

Socrates, G. (1994). *Infrared characteristic group frequencies.* Chichester: Wiley, 11.

U.S. Pharmacopeia, X., US Pharmacopeial Convention, Rockville, 2002, 2011–2012.

Vippagunta, S. R., Brittain, H. G., & Grant, D. J. W. (2001). Crystalline solids. *Ad. Drug Deliv. Rev.*, *48*, 3–26.

Werner, P.-E. (1969). A fortran program for least-squares refinement of crystal structure dimensions. *Arkiv Kemi*, *31*, 513–516.

Werner, P.-E., Eriksson, L., & Westdahl, M. (1985). Treor, a semi-exhaustive trial-and-error powder indexing program for all symmetries. *J. Appl. Crystallography.*, *18*, 108–113.

Woolley, M. L., Marsden, C. A., & Fone, K. C. (2004). 5-HT-$_6$ receptors. *Curr. Drug Target CNS Neurol. Disord.*, *3*, 59–79.

Zhu, H., Yuen, C., & Grant, D. J. (1996). Influence of water activity in organic solvent + water mixtures on the nature of the crystallizing drug phase. 1. Theophylline. *Int. J. Pharm.*, *135*, 151–160.

Zhu, H., & Grant, D. J. (1996). Influence of water activity in organic solvent + water mixtures on the nature of the crystallizing drug phase. 2. Ampicillin. *Int. J. Pharm.*, *139*, 33–43.

Zhu, H., Khankari, R. K., Padden, B. E., Munson, E. J., Gleason, W. B., & Grant, D. J. W. (1996). Physicochemical characterization of nedocromil bivalent metal salt hydrates. 1. Nedocromil magnesium. *J. Pharm. Sci.*, *85*, 1026–1034.

Zhu, H., Padden, B. E., Munson, E. J., & Grant, D. J. W. (1997a). Physicochemical characterization of nedocromil bivalent metal salt hydrates. 2. *Nedocromil zinc J. Pharm. Sci.*, *86*, 418–429.

Zhu, H., Halfen, J. A., Young, V. G., Padden, B. E., Munson, E. J., Menon, V., & Grant, D. J. W. (1997b). Physicochemical characterization of nedocromil bivalent metal salt hydrates. 3. *Nedocromil calcium J. Pharm. Sci.*, *86*, 1439–1447.

Zografi, G. (1998). States of water associated with solids. *Drug Dev. Ind. Pharm.*, *14*, 1905–1926.